Metabolic Engineering 69 (2022) 50–58

Contents lists available at ScienceDirect

Metabolic Engineering

journal homepage: www.elsevier.com/locate/meteng

Adaptive laboratory evolution for improved tolerance of isobutyl acetate in *Escherichia coli*

Morgan M. Matson [a], Mateo M. Cepeda [a], Angela Zhang [a], Anna E. Case [a], Erol S. Kavvas [b], Xiaokang Wang [b,c], Austin L. Carroll [a], Ilias Tagkopoulos [b,d], Shota Atsumi [a,*]

[a] Department of Chemistry, University of California, Davis, CA, 95616, USA
[b] Genome Center, University of California, Davis, CA, 95616, USA
[c] Department of Biomedical Engineering, University of California, Davis, CA 95616, USA
[d] Department of Computer Science, University of California, Davis, CA, 95616, USA

ARTICLE INFO

Keywords:
Adaptive laboratory evolution
Tolerance
Genome sequencing
Esters
Metabolic engineering

ABSTRACT

Previously, *Escherichia coli* was engineered to produce isobutyl acetate (IBA). Titers greater than the toxicity threshold (3 g/L) were achieved by using layer-assisted production. To avoid this costly and complex method, adaptive laboratory evolution (ALE) was applied to *E. coli* for improved IBA tolerance. Over 37 rounds of selective pressure, 22 IBA-tolerant mutants were isolated. Remarkably, these mutants not only tolerate high IBA concentrations, they also produce higher IBA titers. Using whole-genome sequencing followed by CRISPR/Cas9 mediated genome editing, the mutations (SNPs in *metH*, *rho* and deletion of *arcA*) that confer improved tolerance and higher titers were elucidated. The improved IBA titers in the evolved mutants were a result of an increased supply of acetyl-CoA and altered transcriptional machinery. Without the use of phase separation, a strain capable of 3.2-fold greater IBA production than the parent strain was constructed by combing select beneficial mutations. These results highlight the impact improved tolerance has on the production capability of a biosynthetic system.

1. Introduction

Microbial production has emerged as a promising alternative to traditional petroleum-dependent industries and natural extraction processes. Microbes can be engineered to produce a diverse variety of bioactive and industrially relevant chemicals from renewable feedstocks, such as sugars and CO_2 (Case and Atsumi, 2016; Keasling et al., 2021; Pontrelli et al., 2018; Sheng et al., 2020; Sun and Alper, 2020; Yang et al., 2021). The bioproduction of esters has been of particular interest due to their versatile commercial applications as flavorants, fragrances, solvents, coatings, and paints (Carroll et al., 2016). A promising target ester is isobutyl acetate (IBA), a volatile, fruity smelling compound with great potential as a drop-in biofuel. Compared to similar alcohols fuels, such as isobutanol (ISO), IBA's higher volatility and lower polarity and hygroscopicity allow it to be more easily separated from aqueous cell cultures (Rodriguez et al., 2014). These properties, along with its ubiquitous use in the fragrances and food industries, make IBA a valuable commodity chemical and have driven efforts to produce the compound biologically.

Previously, an efficient IBA production pathway was constructed in *E. coli* (Fig. 1) (Rodriguez et al., 2014; Tashiro et al., 2015). This pathway utilizes an alcohol-*O*-acyltransferase (ATF) (Verstrepen et al., 2003) enzyme that condenses acetyl-CoA and ISO, derived from the 2-keto acid-based pathway (Atsumi et al., 2008b), to form IBA (Rodriguez et al., 2014; Tai et al., 2015). A major challenge of biological IBA production is its inherent toxicity. The production strain JCL260 (Atsumi et al., 2008a), previously modified for ISO production, experiences severe growth-inhibition at 3 g/L IBA. This drastically limits titers unless IBA is separated from the culture, such as by removal from the headspace via gas-stripping or from the media via extraction using an organic bilayer. Using hexadecane as a bilayer and an orthogonal acetate assimilating pathway for increased acetyl-CoA generation, titers (20 g/L) greater than the toxicity threshold (3 g/L) were achieved (Tashiro et al., 2015). While these systems greatly increase IBA titers, they also introduce greater production costs and complexities to large scale production. One potential solution to IBA toxicity lies in its low water solubility. At ~8 g/L, IBA innately forms a bilayer in aqueous solutions (Riemenschneider, 2000). Therefore, production utilizing

* Corresponding author.
E-mail address: satsumi@ucdavis.edu (S. Atsumi).

https://doi.org/10.1016/j.ymben.2021.11.002
Received 14 August 2021; Received in revised form 14 October 2021; Accepted 4 November 2021
Available online 8 November 2021

natural bilayer formation is theoretically possible if *E. coli* can be adapted to grow under saturating IBA conditions.

ALE is a powerful tool for optimizing strain tolerance against environmental stressors (Dragosits and Mattanovich, 2013; Lee and Kim, 2020; Portnoy et al., 2011). Through adaptation, desired phenotypes are achieved through the accumulation of mutations overtime to cope with a selective pressure, such as toxicity. These mutations result in improved cellular fitness under stress typically by changing gene expression, altering enzyme function, or re-wiring regulation (Conrad et al., 2011). Often, these changes are synergistic combinations that would otherwise be inaccessible or overlooked by rational design. Previously, ALE has been used to alleviate toxicity for several compounds in various organisms, including ethanol (Yomano et al., 1998), 3-hydroxypropionic acid (Nguyen-Vo et al., 2019) and ISO (Atsumi et al., 2010) in *E. coli*, propionic acid (Xu et al., 2019) in *Saccharomyces cerevisiae*, and *p*-coumaric and ferulic acid (Mohamed et al., 2020) in *Pseudomonas putida* KT2440. These cases highlight the power and versatility of ALE for the overproduction of toxic commodities in microbial hosts.

In this study, an ALE serial transfer method was employed to evolve the ISO production host strain, JCL260, and subsequently 22 IBA-tolerant mutants, M01-23, were isolated. Excitingly, these evolved mutants also demonstrated increased IBA titers without the use of phase separation. To elucidate the mutations beneficial to tolerance and production, the entire genomes of JCL260 and M01-23 were sequenced. The identified mutations were reconstructed individually and in combination in JCL260 to test for enhanced tolerance and production. The *metH, rho,* and *arcA* mutation combination alleviated IBA toxicity while the *metH, rho* combination significantly boosted titers. These reconstructed strains were capable of better tolerance and higher production, respectively, than the evolved strains.

2. Methods

2.1. Reagents

All enzymes were purchased from New England Biolabs. All antibiotics were purchased from MilliporeSigma. All synthetic oligonucleotides were ordered from Integrated DNA Technologies. Sanger sequencing was performed by Genewiz. All chemicals were purchased from MilliporeSigma.

2.2. Strains and plasmids

All strains in this study are listed in Table S1. JCL260 was used as the base strain for ALE. All plasmids and oligonucleotides used in this study are listed in Tables S2 and S3, respectively. Plasmids for IBA production and acetate assimilation were constructed using sequence and ligation independent cloning (SLIC, Table S4) (Li and Elledge, 2007). The constructed plasmids were verified by sequencing.

Genomic modifications were constructed using CRISPR-Cas9-mediated homologous recombination (Jiang et al., 2015). Donor DNA repair fragments for genomic modifications were constructed by PCR assembly or amplification from genomic DNA using primers listed in Tables S3 and S5. Plasmids encoding sgRNAs for CRISPR-Cas9-mediated homologous recombination were constructed with Q5 site-directed mutagenesis (NEB) using pTargetF (Addgene plasmid # 62226) as a template. Primer sets and templates used for plasmid construction are listed in Table S6. All genomic modifications were PCR and sequence verified.

2.3. Culturing

Overnight cultures were grown in 3 ml Luria broth (LB) media containing appropriate antibiotics. Antibiotic concentrations were as follows: kanamycin (50 μg ml^{-1}), ampicillin (200 μg ml^{-1}), tetracycline (20 μg ml^{-1}). IBA selection and tolerance were carried out in M9P medium (33.7 mM Na_2HPO_4, 22 mM KH_2PO_4, 8.6 mM NaCl, 9.4 mM NH_4Cl, 2 mM $MgSO_4$, 0.1 mM $CaCl_2$) including 5 g/L yeast extract (Research Products International); 10 g/L glucose (Fisher BioReagents); 1000 × A5 trace metal mix (2.86 g H_3BO_3, 1.81 g $MnCl_2{\cdot}4H_2O$, 0.079 g $CuSO_4{\cdot}5H_2O$, 49.4 mg $Co(NO_3)_2{\cdot}6H_2O$ per liter water). IBA production was carried out in the same M9P medium except supplemented with 50 g/L glucose. Optical densities were measured at 600 nm (OD_{600}) with a Synergy H1 hybrid plate reader (BioTek Instruments, Inc.).

2.4. ALE for IBA tolerance

An overnight culture of JCL260 was used to inoculate three 15 mL screw cap tubes at a starting OD_{600} of 0.1 in 5 mL of M9P media supplemented with 1.5 g/L IBA. Cultures were grown at 37 °C, 250 rpm for 24 h then OD_{600} was taken. Out of three tubes, the culture with the highest OD_{600} was chosen as the inoculum for the next round of selection. If the culture OD_{600} exceeded 1.0, the concentration of IBA used in next round of selection was increased by 0.05–0.1 g/L. To isolate evolved mutants, cultures were struck onto M9P media plates containing 3.2 g/L IBA and the resulting colonies were designated with M#. After 22 rounds of selection with JCL260 as the inoculum, M01-07 were isolated. P1 phage transduction (Thomason et al., 2007) was carried out on M01-07 pooled with JCL260, followed by 5 rounds of selection and an additional P1 phage transduction. This resulted in M08. Using M08 as the inoculum, 10 rounds of selection resulted in M09-23.

2.5. Genome sequencing and data analysis

The genomic DNA of JCL260 and M01-23 was purified by Qiagen Blood and Cell Culture DNA Mini Kit. Whole-genome sequencing was performed by the Joint Genome Institute (JGI Proposal ID: 503669, NCBI Project ID: JCL260, 537595; EM1-23, 537607–537838). The sequenced JCL260 parental strain was aligned to the BW25113 genome (GenBank: CP009273.1) using *breseq* (Deatherage and Barrick, 2014) to

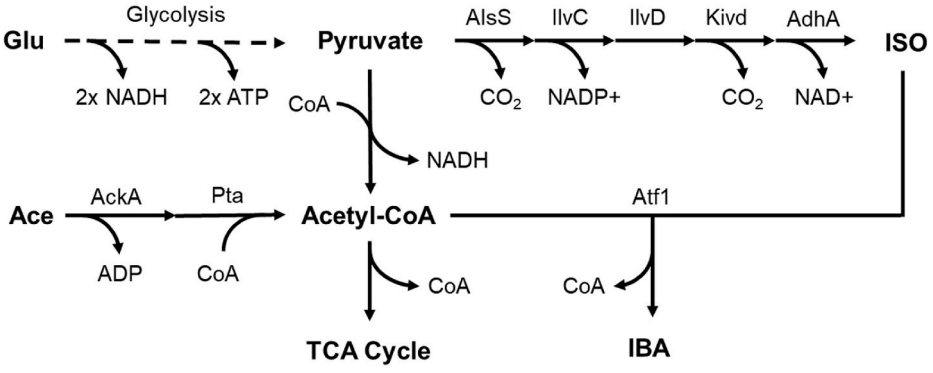

Fig. 1. IBA Production from glucose and acetate in *E. coli*. Ace, acetate; AckA from *E. coli*, acetate kinase; AdhA, alcohol dehydrogenase from *Lactococcus lactis*; AlsS, acetolactate synthase from *Bacillus subtilis*; Atf1, alcohol-*O*-acetyl transferase from *Saccharomyces cerevisiae*; Glu, D-glucose; IBA; isobutyl acetate; IlvC, 2-hydroxy-3-ketol-acid reductoisomerase from *E. coli*; IlvD, dihydroxy-acid hydratase from *E. coli*; ISO, Isobutanol; Kivd, 2-keto acid decarboxylase from *L. lactis*; Pta, phosphate acetyltransferase from *E. coli*.

generate a reference sequence for downstream alignments. In addition to predicted mutations, the generated reference sequence includes *breseq* mutations described as unassigned junction evidence. The sequences of the 22 evolved mutants were then aligned to the reference sequence using *breseq*, which resulted in mutation predictions for each evolved strain. The sequences of the 22 evolved mutants were also aligned to an *E. coli* F plasmid (NCBI Reference Sequence: NC_002483.1). For all alignments involving evolved strains, *breseq* mutations described as unassigned junction evidence were not included in the set of analyzed mutations.

2.6. Tolerance assays

Overnight cultures grown in LB media were centrifuged at 6000 g for 1 min and the supernatant was discarded. The cell pellets were resuspended with M9P media. The concentrated cells were inoculated at an OD_{600} 0.1 into 5 mL of M9P media, containing various concentrations of the target chemical in Parafilm-wrapped 15 mL screw-cap test tubes. Media supplemented with acetic acid were pH adjusted to 7 with 5 M KOH. Cells were incubated at 37 °C, 250 rpm. OD_{600} readings were taken at 24 h.

2.7. Fluorescence assays

Overnight cultures were inoculated at 1% in 3 mL of LB media. Cells were grown to an OD_{600} of 0.4–0.6 at 37 °C, 250 rpm then induced with 1 mM IPTG. The cultures were grown at 37 °C, 250 rpm, for 24 h. Fluorescence emission was measured at 510 nm and with a Synergy H1 hybrid plate reader (BioTek Instruments, Inc.).

2.8. Production

Overnight cultures grown in LB media were inoculated at 1% in 20 mL of M9P in 250 mL screw-cap baffle flasks. Cells were grown to an OD_{600} of 0.4–0.6 at 37 °C, 250 rpm then induced with 1 mM IPTG and if applicable, supplemented with 10 g/L acetate, 1.7 g/L IBA, or 5 g/L ISO. The cultures were wrapped in Parafilm then grown at 30 °C, 250 rpm for the duration of the experiment.

2.9. Gas chromatography analysis

Concentrations of ISO and IBA were analyzed by GC–FID. The GC system is a GC-2010 with an AOC-20 S auto sampler and AOC-20i auto injector (Shimadzu). The column used was a DB-WAX capillary column (30 m length, 0.32 mm diameter and 0.5 μm film thickness; Agilent Technologies). The GC oven temperature was held at 225 °C, and the FID was held at 330 °C. The injection volume was 0.5 μl, injected at a 15:1 split ratio. Helium was used as the carrier gas. Retention times from samples were compared with standards.

To prepare samples for GC analysis, 1 ml of cell culture was centrifuged at 20,000 *g* for 10 min at 4 °C. 100 μL of culture supernatant was diluted with 900 μL MilliQ water.

2.10. Glucose and acetate analysis by high performance liquid chromatography

Concentrations of acetate and glucose were analyzed by 20A HPLC (Shimazu) equipped with a differential refractive detector 10A and an Aminex fast acid analysis column (Bio-Rad). The mobile phase was 5 mM of H_2SO_4, maintained at a flow rate of 0.6 ml min^{-1} at 65 °C for 12.5 min.

To prepare samples for HPLC analysis, 1 mL of cell culture was centrifuged at 20,000g for 10 min at 4 °C. 40 μL of filtered culture supernatant was injected into the column for analysis.

3. Results

3.1. Adaptive laboratory evolution and characterization of the evolved mutants

JCL260 (Atsumi et al., 2008b), previously constructed for high ISO production, was chosen as the parent strain for evolution. JCL260 experiences severe growth-inhibition at 3 g/L IBA (Fig. 2b). To improve JCL260's tolerance towards IBA, a serial transfer method (Yomano et al., 1998) was employed where inoculated M9P media was supplemented with 1.5 g/L IBA and for each subsequent round the surviving culture was diluted into fresh media supplemented with gradually increasing concentrations of IBA (Fig. 2a). After 22 rounds, the seven largest colonies were isolated on an LB agar plate containing 3.2 g/L IBA and designated M01-07. To assess the impact of ALE on tolerance and production in the evolved mutants, M01 was randomly selected for initial screening. After sequencing the genome (details in 3.3), M01 was found to be closely genetically identical to M02-07.

JCL260 and M01 were cultured in the presence of 2, 3, and if relevant, 4 and 5 g/L IBA to evaluate tolerance. Compared to JCL260, M01 showed increased growth in the absence of IBA and presence of 2 and 3 g/L IBA, slight growth at 4 g/L IBA, and no growth at 5 g/L IBA (Fig. 2b). To determine if ALE affected IBA production, JCL260 and M01 harboring the IBA production plasmids, pAL603 ($P_L$lacO$_1$:*alsS-ilvCD*, $P_L$lacO$_1$:*kivd-adhA*; Table S2) and pAL685 ($P_L$lacO$_1$:*ATF1*, Table S2), were cultured in the absence of a solvent layer. This resulted in no ISO or IBA production in M01. To test gene expression under the control of $P_L$lacO$_1$, pAL682 ($P_L$lacO$_1$:*mRFP1* encoding a red fluorescence protein; Table S2) was introduced into JCL260 and M01. In the absence of IPTG, $P_L$lacO$_1$ was tightly repressed in JCL260 but not well repressed in M01 (Fig. S1). These results suggest a loss of repression for $P_L$lacO$_1$ in M01 (Fig. S1). It is well documented that plasmids with leaky expression suffer from instability, wherein the plasmid is maintained through cell proliferation but accumulates mutations that inactivate its genes (Saleski et al., 2021; Tyo et al., 2009). This is especially true for plasmids harboring genes responsible for toxic metabolites (Gruber et al., 2008), like the ISO and IBA pathway genes. The insufficient lac repression in M01 resulted in constitutive expression of the $P_L$lacO$_1$ controlled pathway genes, which likely triggered the loss of ISO and IBA production to avoid considerable growth burden or death during culturing.

To re-establish lac repression in M01, *lacI*^{q} was incorporated into pAL685, generating pAL1114 (Table S2). With the additional repression, M01 was able to produce 2.6 ± 0.1 g/L IBA, a 2.2-fold improvement over JCL260 which produced 1.2 ± 0.1 g/L (Fig. 2c). Conversely, JCL260 produced more ISO than M01, 8.6 ± 0.2 g/L and 4.4 ± 0.3 g/L respectively (Fig. 2c). IBA production relies on the condensation of ISO and acetyl-CoA (Fig. 1). Previously, it was shown that a lower ISO to IBA ratio corresponds to enhanced acetyl-CoA generation facilitating increased flux towards IBA (Rodriguez et al., 2014; Tashiro et al., 2015).

Genome shuffling (Gong et al., 2009), a powerful method to remove non-essential or deleterious mutations while generating novel combinations of beneficial mutations, was subsequently implemented. For recombination, M01-07 was pooled with JCL260 and transduced with P1 phage (Thomason et al., 2007). The resulting colonies were combined and used as inoculum for 5 rounds of selection starting at 3.2 g/L IBA, which was followed by another transduction (Fig. 2a). This resulted in the evolved strain M08. Compared to M01, M08 exhibited similar growth at 2 g/L, reduced growth at 3 g/L and severe growth inhibition at 4 g/L (Fig. 2b). Although M08 exhibited worse tolerance than M01, it produced more IBA, 3.1 ± 0.1 g/L, and had a lower ISO to IBA ratio (Fig. 2c). ALE was resumed with M08 as the inoculum. After 10 rounds starting at 3.4 g/L IBA, M09-23 were isolated and M20 was randomly selected for initial screening. After sequencing the genome (details in 3.3), M20 was found to be closely genetically identical to M09-23. The growth of M08 and M20 were similar at all concentrations of IBA, but M20 produced 3.4 g/L ± 0.0 IBA, a 2.8-fold improvement over JCL260

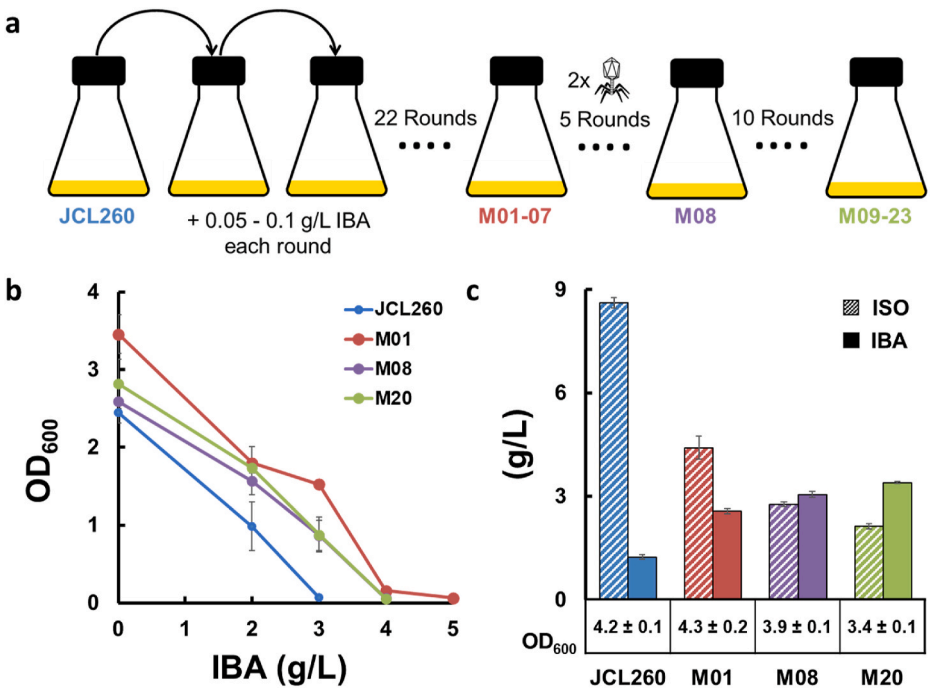

Fig. 2. Adaptive laboratory evolution to improve IBA tolerance. (a) ALE experimental design and chronicle of evolution. Starting at 1.5 g/L IBA in M9P media, surviving cultures were inoculated into fresh media with increasing IBA concentrations, 0.05–0.1 g/L, every round. M01-07 were isolated after 22 rounds. M08 was isolated after two P1 phage transductions and 5 rounds starting at 3.2 g/L IBA. M09-23 were isolated after the final 10 rounds starting at 3.4 g/L IBA. **(b)** JCL260, M01, M08 and M20 were inoculated at OD_{600} 0.1 into 5 mL of M9P media containing 2, 3, and where relevant, 4 and 5 g/L IBA. OD_{600} was measured after 24 h. **(c)** IBA production (solid), ISO production (pattern) and final OD_{600} of JCL260, M01, M08 and M20 cultured in M9P media after 24 h. N = 3 or more, biological replicates; error bars represent s.d.

(Fig. 2c). It is important to note that production above the toxicity threshold (3 g/L) was previously only achievable using phase separation. M20 had the lowest ISO to IBA ratio of all strains. In summary, ALE was successful at increasing IBA tolerance with the added benefit of higher production titers.

3.2. Further characterization of evolved mutant M20

To better understand the phenotypic changes that arose from ALE it was necessary to probe the production capabilities of the evolved mutants. As the highest producing mutant among the strains initially screened, M20 was chosen for these studies. First, it was determined that JCL260 and M20 harboring only the ISO pathway produce the same ISO titers, although the final cell density of M20 was much higher (Fig. S2). The denser growth of M20 may be a result of increased intracellular acetyl-CoA supply, as acetyl-CoA is the primary metabolite for growth and biomass formation in *E. coli* (Fig. 1). To examine acetyl-CoA generation in the two strains, the conversion of 5 g/L ISO to IBA was monitored in JCL260 and M20 harboring only *ATF1*. JCL260 plateaued at 38% conversion (2.1 ± 0.1 g/L IBA) at 8 h whereas M20 achieved 57% conversion (3.0 ± 0.1 g/L IBA) by 10 h (Fig. 3a). The ability to produce more IBA from the same amount of ISO further supports M20 having a larger acetyl-CoA supply. Additionally, the two strains had the same final cell density, suggesting in the presence of ATF1 M20 utilizes acetyl-CoA for IBA production instead of enhancing growth.

Next, it was critical to gauge how the two strains respond to an enhanced acetyl-CoA supply. However, CoA thioesters are not natively transported across *E. coli*'s outer membrane (Black and DiRusso, 2003), which prevents directly supplementing the cultures with exogenous acetyl-CoA. Instead, intracellular acetyl-CoA was increased via acetate assimilation (Tashiro et al., 2015). The acetate kinase–phosphotransacetylase pathway plasmid, pAL956 ($P_L$lacO_1:*ackA-pta*; Table S2), was introduced along with the IBA production pathway plasmids into JCL260 and M20. After culturing the strains for 24 h with 50 g/L glucose and 10 g/L acetate, JCL260 produced 3.1 ± 0.1 g/L IBA and consumed 29% of the glucose and 23% of the acetate whereas M20 produced 3.8 g/L ± 0.2 IBA and consumed 28% of the glucose and only 11% of the acetate (Fig. 3bc). With acetate feeding, JCL260 closely matched the production profile of M20, suggesting acetyl-CoA was previously limiting for production (Fig. 3bc). Interestingly, using less acetate M20 was able to produce slightly more IBA than JCL260. These results strongly indicate that M20 has enhanced acetyl-CoA generation from glucose, facilitating higher IBA production. Subsequently, the intracellular acetyl-CoA supply was measured in both strains, and it was shown that M20 has 2.6-fold greater acetyl-CoA than JCL260 (Fig. S3).

Lastly, it was important to test the effect of IBA stress during growth and production for JCL260 and M20. To do so, 1.7 g/L IBA was added into the production media at induction. Under IBA stress, JCL260 showed a severe 68% decrease in ISO production whereas M20 had no decrease (Fig. 3d). For both strains, the addition of IBA resulted in comparable decreases to IBA production (~30%) and final cell density (~15%). In the presence and absence of IBA, M20 maintained higher IBA titers compared to JCL260. These results suggest the increased acetyl-CoA supply seen in M20 is maintained under IBA stress and, in the presence of both the ISO pathway and ATF1, is siphoned from growth and biomass formation for IBA production.

3.3. Whole genome sequencing and analysis of evolved strains

To identify the beneficial mutations associated with improved tolerance and higher titers, the genomes of M01-23 and JCL260 were sequenced. Using *breseq* (Deatherage and Barrick, 2014), the evolved mutant reads were aligned to both JCL260 and the *E. coli* reference genome sequence, BW25113 (Table S1). This allowed for the identification of genetic mutations that arose during ALE (Fig. 4, Table S5). M01-07 were found to have four primary mutations, two single-nucleotide polymorphisms (SNPs) in *rho* and *metH*, one IS30 insertion into *yjjY*, and one deletion in $lacI^q$ on F'. Two other mutations found, an intergenic mutation and insertion, did not carry forward in ALE, suggesting they do not benefit tolerance and production. M08 was found to have four additional mutations, three SNPs in *cysP*, *dctA*, and *yiiR* and one deletion including and in between *yahI* and *mhpC* (Fig. 4, Table S7). M09-23 had one additional conserved mutation, an intergenic insertion between *glmU* and *mhpC*. Mutations that persisted through ALE (*rho*, *metH*, *cysP*, *dctA*, *yiiR* SNPs, $lacI^q$ and *yahI-mhpC* deletions, *glmU/mhpC* indel, and IS30 insertion in *yjjY*) were targeted for further analysis.

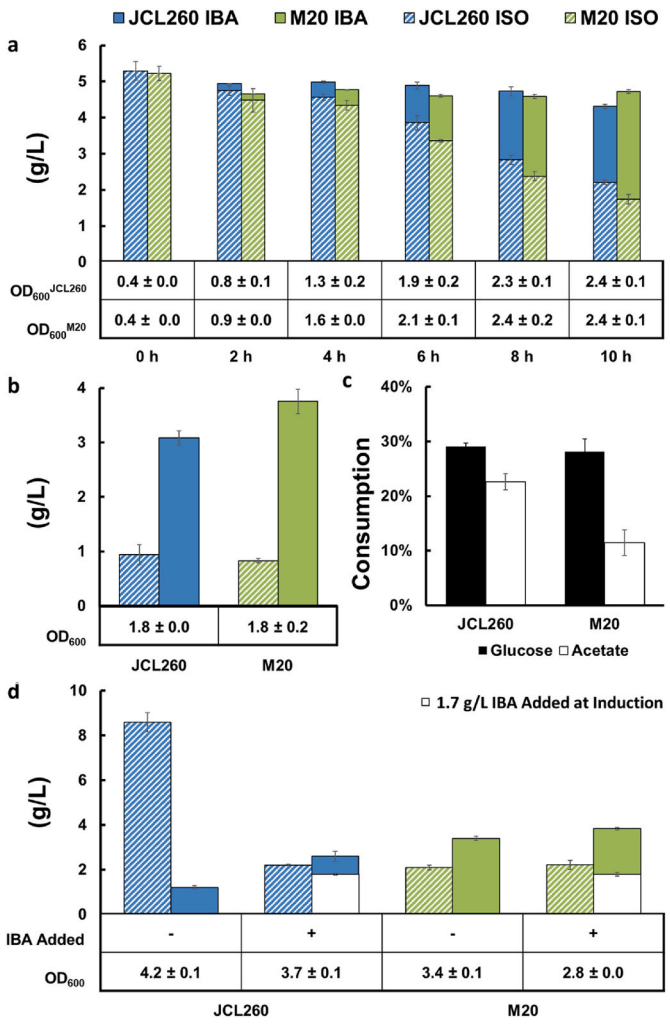

Fig. 3. ISO and IBA production from JCL260 and M20 under various conditions. (a) IBA production (solid), ISO consumption (pattern), and final OD_{600} in M9P media with 5 g/L ISO added at induction. **(b–c)** IBA Production with acetate feeding. JCL260 and M20 with the IBA biosynthetic and acetate assimilation pathways were grown in M9P media with 50 g/L glucose and 10 g/L acetate. **(b)** IBA production (solid), ISO production (pattern) and OD_{600} after 24 h. **(c)** Glucose and acetate consumption. **(d)** IBA production (solid), ISO production (pattern) and OD_{600} after 24 h cultured in M9P media with and without 1.7 g/L IBA added at induction. N = 3, biological replicates; error bars represent s.d.

3.4. CRISPR/Cas9 mediated M20 reversion

An efficient method to identify beneficial mutations is reversion, wherein the reversion of a beneficial mutation to wildtype would result in decreased tolerance and/or production. The M20 mutant contains all the conserved ALE mutations, hence was chosen for reversion. Repair of the SNPs was attempted in M20 (*rho*, *metH, yiiR*, *cysP,* and *dctA*) using a CRISRP/Cas9 method (Jiang et al., 2015). Unfortunately, the modifications failed, likely due to the complete loss of lac repression in M20 (Fig. S1). The CRISPR system used relies on a lac promoter, P_{trc} (Brosius et al., 1985), to control plasmid curing mechanisms (Table S2). Stepwise reconstruction of the mutations in JCL260 was chosen as an alternative to M20 reversion.

3.5. Construction and characterization of M01-07 mutations

To identify the mutations responsible for improved IBA tolerance and increased IBA titers in strains M01-07, the *metH*, *rho*, *ΔarcA*, and Δ*lac* mutations were introduced individually and in combination in JCL260 using CRISPR/Cas9 (Jiang et al., 2015) (Table S1, S5-7). The *metH* and *rho* SNPs were reconstructed with the addition of non-codon altering PAM scrambles in which either G in the NGG sequence was changed to avoid recognition by Cas9. The IS30 insertion in *yjjY* and the $lacI^q$ deletion required more nuanced genetic manipulations. Inserted near the start codon of *yjjY*, the IS30 sequence contains terminators at each end that reduce the expression of genes both upstream and downstream of the insertion site (Dalrymple and Arber, 1986). The *yjjY* gene is located between *ParcA* and *arcA*. The IS30 terminators in the *ParcA*:*arcA* reading frame are particularly strong, permitting less than 2% expression in downstream genes from external promoters (Dalrymple and Arber, 1986). Therefore, the IS30 insertion should disrupt *yjjY* expression and strongly reduce the expression of *arcA* from *ParcA* (Fig. S4). Although duplication of the IS30 insertion was attempted using CRISRP/Cas9 in JCL260 several times, construction of the mutant failed. Instead, to mimic the loss of *yjjY* and *arcA* expression, the entire loci (Δ*arcA-yjjY-ParcA,* denoted Δ*arcA*) was deleted. $lacI^q$ is located on the F′ plasmid, which is closely identical to the genome in the region of interest, therefore preventing either site to be targeted individually. Hence, the entire lac operon (Δ*lac*) on both the genome and F' plasmid had to be knocked out simultaneously to emulate Δ$lacI^q$.

The constructed individual and combined mutants were treated with 3 g/L IBA for 24 h (Fig. 5a). JCL260 and M01, which contains all the conserved ALE mutations from M01-M07, were used as benchmarks for improvement. All strains had identical growth in the absence of IBA. No individual mutant showed improved tolerance compared to JCL260. Conversely, all the combined mutants demonstrated better tolerance than JCL260. The *metH*, *rho*, *ΔarcA* triple mutant had the best tolerance phenotype, with a 1.7-fold higher final cell density than M01. Next, the effects of each mutant on IBA production were examined (Fig. 5b). The *metH* and *rho* single mutants showed increased IBA titers relative to M01, with the *metH*, *rho* double mutant having the highest IBA titer at 4 ± 0.1 g/L. This represents a 1.5-fold improvement over M01 (2.6 g/L ± 0.1 IBA), 1.2-fold improvement over M20 (3.4 ± 0.0 g/L IBA), and a remarkable 3.2-fold improvement over JCL260 (1.2 g/L ± 0.1 IBA). All mutant strains containing *ΔarcA* showed a decrease in IBA production.

3.6. Tolerance to other stressors

To test if the most IBA tolerant strain (*metH*, *rho*, *ΔarcA*) also showed improved tolerance to other chemical stressors, JCL260 and the triple mutant were cultured in the presence of propyl acetate, octanoic acid, acetic acid, ISO, and 3-methyl-1-butanol. Interestingly, compared to JCL260 the triple mutant showed improved tolerance towards acetate esters and acids, but not higher chain alcohols (Fig. 6).

3.7. Construction and characterization of M08-23 mutations

To identify the mutations responsible for the improved IBA titers in strains M08-23, the *cysP*, *dctA, yiiR*, and Δ*yahI-mhpC* mutations were introduced in combination with the *metH*, *rho*, and *ΔarcA* mutations using CRISPR/Cas9 (Jiang et al., 2015) (Fig. 4, Table S1&7). The *cysP*, *dctA* and *yiiR* SNPs were reconstructed with the addition of non-codon altering PAM scrambles. The [*yahI*]-*mhpC* deletion (30 Kb) was replicated by knocking out the entire region (denoted Δ*yahI-mhpC*). Each operon within the 30 Kb region was also knocked out individually (Δ*yahIHJKLMNO*, denoted Δ*yah*; Δ*mhpRABC*, denoted Δ*mhp*; Δ*prpRBCDE,* denoted Δ*prp*, Δ*codBA*, denoted Δ*cod*; Δ*cynRTSX*, denoted Δ*cyn*). The lac operon, also located between *yahI-mhpC*, was previously examined (Fig. 5). Despite multiple attempts, replication of the SNP between *glmU* and *atpC* was unsuccessful.

Only the effect of the mutations on IBA production were of interest since the M09-23 mutants demonstrated higher titers, but worse tolerance than the M01-07 mutants. JCL260 and M20, which contains all the conserved ALE mutations, were used as benchmarks for improvement.

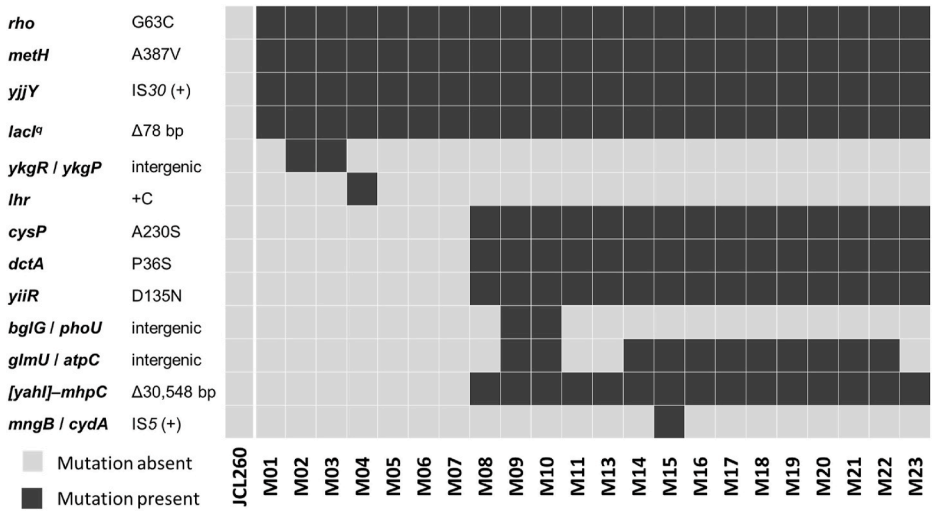

Fig. 4. Overview of mutations in M01-23. Using JCL260 as comparison (grey), we identified mutations present (black) in the evolved strains that arose during ALE. (+) represents forward direction of the IS elements. More detailed information about these mutations is in Table S7.

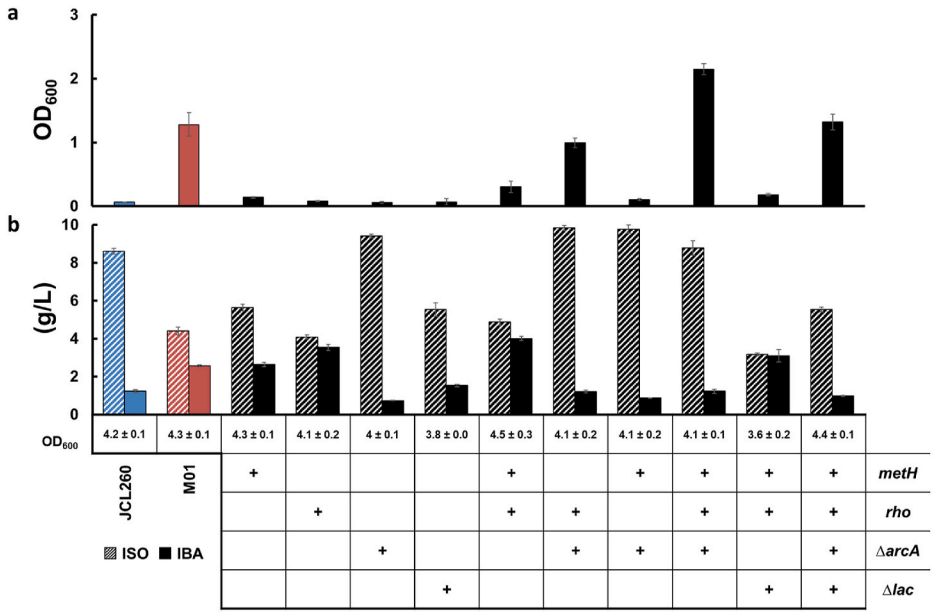

Fig. 5. Effect of M01-M07 mutations on tolerance and IBA production. (a) Strains were inoculated at OD_{600} 0.1 into 5 mL of M9P media containing 3 g/L IBA. OD_{600} was measured after 24 h. **(b)** IBA production (solid), ISO production (pattern) and final OD_{600} of the strains cultured in M9P media after 24 h. N = 3 or more, biological replicates; error bars represent s.d.

The *cysP*, *dctA*, *yiiR* SNPs combination with *metH*, *rho* demonstrated decreased production compared to *metH*, *rho* alone. Similar to previous results (Fig. 5), the addition of *ΔarcA* significantly reduced production (Fig. 7). Neither Δ*yahI-mhpC* or any individual operon deletion, except Δ*lac*, showed improved IBA titers compared to JCL260 (Figs. 7 and S5). No combination of Δ*yahI-mhpC* and its operons with *metH*, *rho*, and/or *ΔarcA* improved titers either (Figs. 7 and S6).

4. Discussion

Here, 22 IBA-tolerant mutants were isolated from ALE and strain reconstruction was used to identify mutations beneficial to tolerance and production. When compared to JCL260, the most IBA tolerant reconstructed strain (*metH*, *rho*, *ΔarcA*) demonstrated no production benefit and the reconstructed strain (*metH, rho*) with the highest IBA titer exhibited only a moderate improvement to tolerance. Understanding how these mutations influence IBA tolerance and production requires insight into the mechanistic effects of IBA toxicity on metabolism. Unfortunately, unlike other toxic byproducts like ethanol, IBA toxicity has not been studied. However, under a microscope, cells treated with 3 g/L IBA are elongated compared to cells grown in the absence of IBA (Fig. S7). Notably, M01 cells appear remarkably longer than JCL260 cells. This suggests IBA inhibits cell division, particularly in the evolved mutants. Cell membrane disruption is a frequent phenomenon seen with toxic and hydrophobic metabolites (Alakomi et al., 2000; Huffer et al., 2011; Royce et al., 2013). Hydrophobic metabolites are more lipid soluble, leading them to interfere with membrane composition and fluidity. This often causes substantial cell morphology modifications, like cell elongation. High concentrations of toxic metabolites are also known to disturb transcriptional machinery and damage DNA (Kang et al., 2016), which trigger stress responses and lead to cell elongation (Wehrens et al., 2018; Wong et al., 2010). These morphology

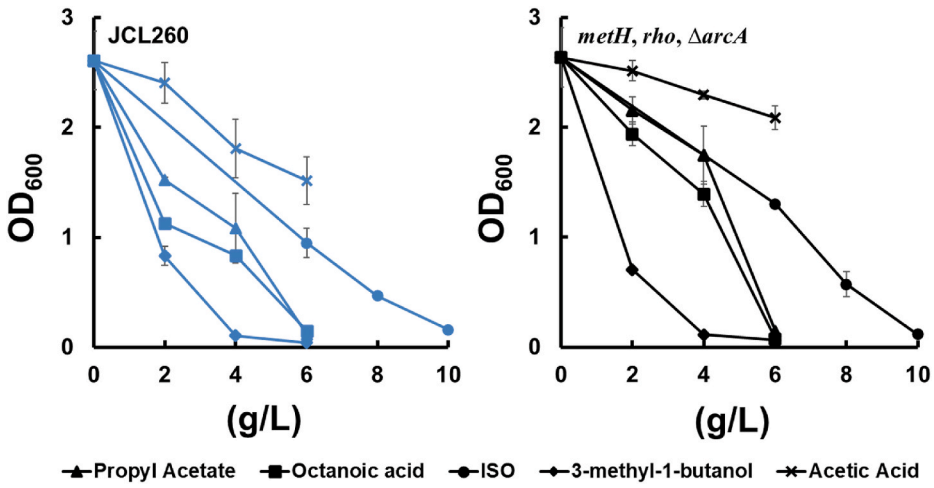

Fig. 6. Toxic effects of various chemicals on JCL260 (left, blue) and the triple mutant *metH, rho, ΔarcA* (right, black). The strains were inoculated at OD_{600} 0.1 into 5 mL of M9P media containing the various chemicals at the indicated concentrations. OD_{600} was measured after 24 h. N = 3 or more, biological replicates; error bars represent s.d. (For interpretation of the references to colour in this figure legend, the reader is referred to the Web version of this article.)

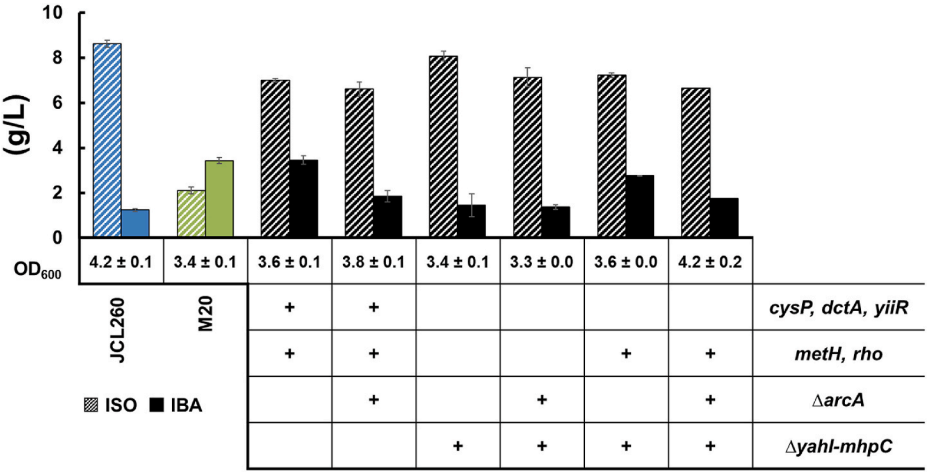

Fig. 7. Effect of M01-M23 mutations on IBA production. IBA production (solid), ISO production (pattern) and OD_{600} of the strains cultured in M9P media after 24 h. N = 3 or more, biological replicates; error bars represent s.d.

changes give key insights into the toxicity mechanisms of IBA.

The ArcA mutation was singularly antipodal in its effects on tolerance and production. ArcA is a transcription regulator that directly or indirectly effects the expression of over 350 genes (Liu and De Wulf, 2004; Salmon et al., 2003). Primarily, ArcA represses genes associated with aerobic metabolism, such as the operons for β-oxidation of fatty acids, the TCA cycle, and glycolate/glyoxylate oxidation (Park et al., 2013). It has been shown that Δ*arcA* results in increased flux to the TCA cycle both in aerobic and anerobic conditions, while only in anerobic or microaerobic conditions does the deletion increase flux towards biomass formation (Nikel et al., 2008; Perrenoud and Sauer, 2005). This may explain why in the microaerobic system used Δ*arcA* improves tolerance but decreases IBA titers (Fig. 5), as acetyl-CoA is diverted from IBA production to growth or biomass generation. Hence, whenever Δ*arcA* was introduced to a strain the titer decreased but cell density increased (Figs. 5 and 7). Interestingly, Δ*arcA* was shown to enhance the production of acetyl-CoA derived products in BL21 strains (Liu and De Wulf, 2004). This is attributed to lower catabolite repression and the presence of the acetyl-CoA synthetase pathway in BL21 strains, which allow for improved acetate assimilation compared to K12 strains.

Inactivated *arcA* also explains the higher glucose utilization and lower acetate utilization seen in M20 (Fig. 3b). Δ*arcA* has been previously shown to increase glycolytic flux and pyruvate dehydrogenase (PDH) levels, the enzyme responsible for the conversion of pyruvate to acetyl-CoA (Nizam et al., 2009; Vemuri et al., 2006). These factors directly improve glucose utilization, allowing for more biomass formation from the same amount of glucose. In *E. coli*, the small RNA SdhX negatively regulates *ackA*, which codes for an enzyme in the reversible acetate kinase–phosphotransacetylase pathway that interconverts acetate and acetyl-CoA (Fig. 1). ShdX binds to the start codon of *ackA* mRNA, consequently blocking translation (De Mets et al., 2019). When *arcA* is deleted, SdhX levels increase which decrease AckA levels, thereby lowering the ability of M20 to assimilate and produce acetate (De Mets et al., 2019; Nikel et al., 2008). This prevents significant carbon loss from acetyl-CoA during fermentation, furnishing more carbon for growth or biomass formation.

Another key mutation found was *rho*, which codes for the Rho transcription terminator factor. Rho is a global regulator of gene expression and has been shown to acutely inhibit PrpCD and CadA (Cardinale et al., 2008). PrpCD are enzymes involved in propionate catabolism and their inhibition results in increased propionyl-CoA levels that subsequently inhibit PDH (Rocco and Escalante-Semerena, 2010). CadA is heavily involved in *E. coli*'s acid stress response (Peng et al., 2014). Previous ALE studies have identified *rho* mutations that confer

improved tolerance towards ethanol and L-serine (Goodarzi et al., 2010; Mundhada et al., 2017), with one study attributing the improved tolerance to reduced Rho activity (Haft et al., 2014). The compromised activity alleviated the effects of premature termination induced by ethanol. If IBA exerts similar effects on *E. coli's* transcriptional machinery, this, along with decrease inhibition of PrpCD and CadA, would explain the role of *rho* in improved tolerance (Fig. 5).

Additionally, diminished Rho activity was shown to increase membrane permeability and upregulate various small molecule transporters (Hafeezunnisa and Sen, 2020). During production, improved efflux of IBA from the cytosol would reduce its intracellular accumulation, therefore decrease the toxic effects of IBA and allow for greater production. Rho inhibition also rendered DNA damage repair in *E. coli* ineffective and resulted in various physiology changes (Jain et al., 2019). Since DNA damage can result in cell elongation (Mo and Burkholder, 2010), this implicates the *rho* mutant in the significant cell elongation seen in M01 under IBA stress. Microscope images confirm *rho* cells appear exceptionally longer than the other strains (Fig. S7). Interestingly, while the *metH*, *rho*, *ΔarcA* triple mutant also displays elongate cells, they do not appear as long as M01 or *rho*. Therefore, *metH* and *ΔarcA* may play a role in recovering the *rho* phenotype. As a global transcription terminator, Rho impacts numerous, non-related areas of metabolism. Thus, further study will be needed to elucidate the precise benefits of the *rho* mutation on IBA tolerance and production.

The final mutation of significance is *metH,* a gene that encodes for a cobalamin-dependent methionine synthase that catalyzes the synthesis of methionine from homocysteine. Although it is unknown if the *metH* mutation (A387V) improves synthase activity, increased intracellular methionine stimulates *E. coli* growth at various temperatures (37–46 °C) and alleviates the toxicity of acetic acid and other weak organic acids (Mordukhova et al., 2008). Methionine acts as a form of negative feedback inhibition on its own biosynthetic pathway, preventing the build-up of its toxic precursor, homocysteine (Tuite et al., 2005). Moreover, various stressors have been shown to halt ribosomes on AUG codons, which limits the availability of methionyl-tRNA^{Met} for protein synthesis (VanBogelen et al., 1987). Enhanced methionine generation was able to alleviate this deficiency (Haft et al., 2014). This study also demonstrated a cooperative effect of increased methionine and reduced Rho activity on alleviating ethanol toxicity by separation of transcription from translation. These factors may explain the synergy seen between *metH*, *rho* for production and ultimately the role of *metH* in improving IBA tolerance (Fig. 5).

In addition to the key mutations above, the *lacI^q* deletion on the F' plasmid and the lac operon deletion located within [*yahI*]-*mhpC* are also of interest. These deletions explain the stepwise loss of lac repression seen in the mutants (Fig. S1). Since *lacI^q* had to be reintroduced into the system to re-establish control over $P_L$lacO$_1$ expression, it is hard to gauge the holistic effect of Δ*lac* on production. Using fluorescence as a guide, the incremental loss of lac repression led to a stepwise increase in mRFP1 expression under $P_L$lacO$_1$ compared to JCL260. This may explain the slight improvement to production titer seen in Δ*lac* (Fig. 5b), as the ISO and IBA pathway genes are also under the control of $P_L$lacO$_1$ (Table S2).

The most IBA tolerant reconstructed strain, *metH*, *rho*, *ΔarcA,* was able to achieve similar growth in the presence and absence of 3 g/L IBA, an otherwise toxic concentration for *E. coli*. Although this tolerance is short of the 8 g/L IBA bilayer goal, further study into how these mutations effect tolerance may pave new avenues for continued improvement. This triple mutant also showed improved tolerance towards acetate esters and acids, but not higher chain alcohols. Curiously, a previous study evolving JCL260 demonstrated deletion of the TolC-efflux system improved ISO tolerance (Atsumi et al., 2010). Reduced Rho activity has been shown to cripple TolC-efflux in *E. coli* (Hafeezunnisa and Sen, 2020), yet no improvement to ISO tolerance was seen in the triple mutant. Likely, multiple mutations to genes induced by the presence of higher alcohols and heavily involved in membrane composition and permeability are required to alleviate the toxic effects of ISO and 3-methyl-1-butanol.

Among the evolved mutants, the strains isolated during late ALE (M08-M22) produced the most IBA. Yet, the reconstructed strain with the highest IBA titer (*metH, rho*) only contained mutations that originated early in ALE (M01-M07). The failure of the M08-23 mutations to improve titer may be due to metabolic discrepancies between the reconstructed and evolved strains. It has been shown that IS30 elements do not completely terminate the activity of neighboring genes, suggesting there may be residual activity of ArcA in the evolved mutants (Dalrymple and Arber, 1986).

5. Conclusion

Product toxicity plays a critical role in the industrial viability of a microbial production system (Dragosits and Mattanovich, 2013). Using ALE, 22 mutant strains capable of increased IBA tolerance and production were isolated. Through individual and combined mutation constructs, the synergistic effects of the mutations on tolerance and production were explored. Through these reconstructions, strains were created with higher titers (*metH*, *rho*) and better tolerance (*metH*, *rho*, *ΔarcA*) than the evolved mutants. Additionally, the most IBA-tolerant strain also showed improved tolerance towards other acetate esters and acids. While these genes have been previously implicated in improved tolerance or production for other metabolites and organisms, further studies are required to understand their mechanistic roles in *E. coli* IBA metabolism.

Author contributions

M.M., A.Z., A.E.C., and S.A. designed research; M.M., M.C., Ap.Z., A. E.C., and A.L.C. performed the experiments; M.M., M.C., A.Z., A.E.C., E. K., X.W., I.T., and S.A. analyzed data; and M.M. and S.A. wrote the paper.

Acknowledgements

This work was supported by a University of California-Davis Chancellor's Fellowship to S.A. Whole-genome sequencing was performed by the Joint Genome Institute (JGI Proposal ID: 503669). M.M. was supported by a UC Davis Innovation Institute for Food and Health Innovator Fellowship. A.Z. was supported by a US National Institutes of Health Training Grant Fellowship (T32-GM113770). We thank Jake Gonzales for critical reading of the manuscript.

Appendix A. Supplementary data

Supplementary data to this article can be found online at https://doi.org/10.1016/j.ymben.2021.11.002.

References

Alakomi, H.L., Skytta, E., Saarela, M., Mattila-Sandholm, T., Latva-Kala, K., Helander, I. M., 2000. Lactic acid permeabilizes gram-negative bacteria by disrupting the outer membrane. Appl. Environ. Microbiol. 66, 2001–2005.

Atsumi, S., Cann, A.F., Connor, M.R., Shen, C.R., Smith, K.M., Brynildsen, M.P., Chou, K. J., Hanai, T., Liao, J.C., 2008a. Metabolic engineering of *Escherichia coli* for 1-butanol production. Metab. Eng. 10, 305–311.

Atsumi, S., Hanai, T., Liao, J.C., 2008b. Non-fermentative pathways for synthesis of branched-chain higher alcohols as biofuels. Nature 451, 86–89.

Atsumi, S., Wu, T.Y., Machado, I.M., Huang, W.C., Chen, P.Y., Pellegrini, M., Liao, J.C., 2010. Evolution, genomic analysis, and reconstruction of isobutanol tolerance in *Escherichia coli*. Mol. Syst. Biol. 6, 449.

Black, P.N., DiRusso, C.C., 2003. Transmembrane movement of exogenous long-chain fatty acids: proteins, enzymes, and vectorial esterification. Microbiol. Mol. Biol. Rev. 67, 454–472.

Brosius, J., Erfle, M., Storella, J., 1985. Spacing of the -10 and -35 regions in the tac promoter. Effect on its *in vivo* activity. J. Biol. Chem. 260, 3539–3541.

Cardinale, C.J., Washburn, R.S., Tadigotla, V.R., Brown, L.M., Gottesman, M.E., Nudler, E., 2008. Termination factor Rho and its cofactors NusA and NusG silence foreign DNA in *E. coli*. Science 320, 935–938.
Carroll, A.L., Desai, S.H., Atsumi, S., 2016. Microbial production of scent and flavor compounds. Curr. Opin. Biotechnol. 37, 8–15.
Case, A.E., Atsumi, S., 2016. Cyanobacterial chemical production. J. Biotechnol. 231, 106–114.
Conrad, T.M., Lewis, N.E., Palsson, B.O., 2011. Microbial laboratory evolution in the era of genome-scale science. Mol. Syst. Biol. 7, 509.
Dalrymple, B., Arber, W., 1986. The characterization of terminators of RNA transcription on IS30 and an analysis of their role in IS element-mediated polarity. Gene 44, 1–10.
De Mets, F., Van Melderen, L., Gottesman, S., 2019. Regulation of acetate metabolism and coordination with the TCA cycle via a processed small RNA. Proc. Natl. Acad. Sci. U. S. A. 116, 1043–1052.
Deatherage, D.E., Barrick, J.E., 2014. Identification of mutations in laboratory-evolved microbes from next-generation sequencing data using breseq. Methods Mol. Biol. 1151, 165–188.
Dragosits, M., Mattanovich, D., 2013. Adaptive laboratory evolution – principles and applications for biotechnology. Microb. Cell Factories 12, 64.
Gong, J., Zheng, H., Wu, Z., Chen, T., Zhao, X., 2009. Genome shuffling: progress and applications for phenotype improvement. Biotechnol. Adv. 27, 996–1005.
Goodarzi, H., Bennett, B.D., Amini, S., Reaves, M.L., Hottes, A.K., Rabinowitz, J.D., Tavazoie, S., 2010. Regulatory and metabolic rewiring during laboratory evolution of ethanol tolerance in *E. coli*. Mol. Syst. Biol. 6, 378.
Gruber, D.F., Pieribone, V.A., Porton, B., Kao, H.T., 2008. Strict regulation of gene expression from a high-copy plasmid utilizing a dual vector system. Protein Expr. Purif. 60, 53–57.
Hafeezunnisa, M., Sen, R., 2020. The Rho-dependent transcription termination is involved in broad-spectrum antibiotic susceptibility in *Escherichia coli*. Front. Microbiol. 11, 605305.
Haft, R.J., Keating, D.H., Schwaegler, T., Schwalbach, M.S., Vinokur, J., Tremaine, M., Peters, J.M., Kotlajich, M.V., Pohlmann, E.L., Ong, I.M., Grass, J.A., Kiley, P.J., Landick, R., 2014. Correcting direct effects of ethanol on translation and transcription machinery confers ethanol tolerance in bacteria. Proc. Natl. Acad. Sci. U. S. A. 111, E2576–E2785.
Huffer, S., Clark, M.E., Ning, J.C., Blanch, H.W., Clark, D.S., 2011. Role of alcohols in growth, lipid composition, and membrane fluidity of yeasts, bacteria, and archaea. Appl. Environ. Microbiol. 77, 6400–6408.
Jain, S., Gupta, R., Sen, R., 2019. Rho-dependent transcription termination in bacteria recycles RNA polymerases stalled at DNA lesions. Nat. Commun. 10, 1207.
Jiang, Y., Chen, B., Duan, C., Sun, B., Yang, J., Yang, S., 2015. Multigene editing in the *Escherichia coli* genome via the CRISPR-Cas9 system. Appl. Environ. Microbiol. 81, 2506–2514.
Kang, Y., Lee, J., Kim, J., Oh, Y., Kim, D., Lee, J., Lim, S., Jo, K., 2016. Analysis of alcohol-induced DNA damage in *Escherichia coli* by visualizing single genomic DNA molecules. Analyst 141, 4326–4331.
Keasling, J., Garcia Martin, H., Lee, T.S., Mukhopadhyay, A., Singer, S.W., Sundstrom, E., 2021. Microbial production of advanced biofuels. Nat. Rev. Microbiol. https://doi.org/10.1038/s41579-021-00577-w.
Lee, S., Kim, P., 2020. Current status and applications of adaptive laboratory evolution in industrial microorganisms. J. Microbiol. Biotechnol. 30, 793–803.
Li, M.Z., Elledge, S.J., 2007. Harnessing homologous recombination *in vitro* to generate recombinant DNA via SLIC. Nat. Methods 4, 251–256.
Liu, X., De Wulf, P., 2004. Probing the ArcA-P modulon of *Escherichia coli* by whole genome transcriptional analysis and sequence recognition profiling. J. Biol. Chem. 279, 12588–12597.
Mo, A.H., Burkholder, W.F., 2010. YneA, an SOS-induced inhibitor of cell division in *Bacillus subtilis*, is regulated posttranslationally and requires the transmembrane region for activity. J. Bacteriol. 192, 3159–3173.
Mohamed, E.T., Werner, A.Z., Salvachua, D., Singer, C.A., Szostkiewicz, K., Rafael Jimenez-Diaz, M., Eng, T., Radi, M.S., Simmons, B.A., Mukhopadhyay, A., Herrgard, M.J., Singer, S.W., Beckham, G.T., Feist, A.M., 2020. Adaptive laboratory evolution of *Pseudomonas putida* KT2440 improves p-coumaric and ferulic acid catabolism and tolerance. Metabol. Eng. Commun. 11, e00143.
Mordukhova, E.A., Lee, H.S., Pan, J.G., 2008. Improved thermostability and acetic acid tolerance of *Escherichia coli* via directed evolution of homoserine *o*-succinyltransferase. Appl. Environ. Microbiol. 74, 7660–7668.
Mundhada, H., Seoane, J.M., Schneider, K., Koza, A., Christensen, H.B., Klein, T., Phaneuf, P.V., Herrgard, M., Feist, A.M., Nielsen, A.T., 2017. Increased production of L-serine in *Escherichia coli* through adaptive laboratory evolution. Metab. Eng. 39, 141–150.
Nguyen-Vo, T.P., Liang, Y., Sankaranarayanan, M., Seol, E., Chun, A.Y., Ashok, S., Chauhan, A.S., Kim, J.R., Park, S., 2019. Development of 3-hydroxypropionic-acid-tolerant strain of *Escherichia coli* W and role of minor global regulator *yieP*. Metab. Eng. 53, 48–58.
Nikel, P.I., Pettinari, M.J., Ramirez, M.C., Galvagno, M.A., Mendez, B.S., 2008. *Escherichia coli arcA* mutants: metabolic profile characterization of microaerobic cultures using glycerol as a carbon source. J. Mol. Microbiol. Biotechnol. 15, 48–54.
Nizam, S.A., Zhu, J., Ho, P.Y., Shimizu, K., 2009. Effects of *arcA* and *arcB* genes knockout on the metabolism in *Escherichia coli* under aerobic condition. Biochem. Eng. J. 44, 240–250.
Park, D.M., Akhtar, M.S., Ansari, A.Z., Landick, R., Kiley, P.J., 2013. The bacterial response regulator ArcA uses a diverse binding site architecture to regulate carbon oxidation globally. PLoS Genet. 9, e1003839.
Peng, S., Stephan, R., Hummerjohann, J., Tasara, T., 2014. Transcriptional analysis of different stress response genes in *Escherichia coli* strains subjected to sodium chloride and lactic acid stress. FEMS Microbiol. Lett. 361, 131–137.
Perrenoud, A., Sauer, U., 2005. Impact of global transcriptional regulation by ArcA, ArcB, Cra, Crp, Cya, Fnr, and mlc on glucose catabolism in *Escherichia coli*. J. Bacteriol. 187, 3171–3179.
Pontrelli, S., Chiu, T.Y., Lan, E.I., Chen, F.Y., Chang, P., Liao, J.C., 2018. *Escherichia coli* as a host for metabolic engineering. Metab. Eng. 50, 16–46.
Portnoy, V.A., Bezdan, D., Zengler, K., 2011. Adaptive laboratory evolution–harnessing the power of biology for metabolic engineering. Curr. Opin. Biotechnol. 22, 590–594.
Riemenschneider, W., 2000. Esters, Organic. Ullmann's Encyclopedia of Industrial Chemistry.
Rocco, C.J., Escalante-Semerena, J.C., 2010. In *Salmonella enterica*, 2-methylcitrate blocks gluconeogenesis. J. Bacteriol. 192, 771–778.
Rodriguez, G.M., Tashiro, Y., Atsumi, S., 2014. Expanding ester biosynthesis in *Escherichia coli*. Nat. Chem. Biol. 10, 259–265.
Royce, L.A., Liu, P., Stebbins, M.J., Hanson, B.C., Jarboe, L.R., 2013. The damaging effects of short chain fatty acids on *Escherichia coli* membranes. Appl. Microbiol. Biotechnol. 97, 8317–8327.
Saleski, T.E., Chung, M.T., Carruthers, D.N., Khasbaatar, A., Kurabayashi, K., Lin, X.N., 2021. Optimized gene expression from bacterial chromosome by high-throughput integration and screening. Sci. Adv. 7.
Salmon, K., Hung, S.P., Mekjian, K., Baldi, P., Hatfield, G.W., Gunsalus, R.P., 2003. Global gene expression profiling in *Escherichia coli* K12. The effects of oxygen availability and FNR. J. Biol. Chem. 278, 29837–29855.
Sheng, H., Sun, X., Yan, Y., Yuan, Q., Wang, J., Shen, X., 2020. Metabolic engineering of microorganisms for the production of flavonoids. Front. Bioeng. Biotechnol. 8, 589069.
Sun, L., Alper, H.S., 2020. Non-conventional hosts for the production of fuels and chemicals. Curr. Opin. Chem. Biol. 59, 15–22.
Tai, Y.S., Xiong, M., Zhang, K., 2015. Engineered biosynthesis of medium-chain esters in *Escherichia coli*. Metab. Eng. 27, 20–28.
Tashiro, Y., Desai, S.H., Atsumi, S., 2015. Two-dimensional isobutyl acetate production pathways to improve carbon yield. Nat. Commun. 6, 7488.
Thomason, L.C., Costantino, N., Court, D.L., 2007. *E. coli* genome manipulation by P1 transduction. Curr. Protoc. Mol. Biol. 79, 1.17.1–1.17.8.
Tuite, N.L., Fraser, K.R., O'Byrne C, P., 2005. Homocysteine toxicity in *Escherichia coli* is caused by a perturbation of branched-chain amino acid biosynthesis. J. Bacteriol. 187, 4362–4371.
Tyo, K.E., Ajikumar, P.K., Stephanopoulos, G., 2009. Stabilized gene duplication enables long-term selection-free heterologous pathway expression. Nat. Biotechnol. 27, 760–765.
VanBogelen, R.A., Kelley, P.M., Neidhardt, F.C., 1987. Differential induction of heat shock, SOS, and oxidation stress regulons and accumulation of nucleotides in *Escherichia coli*. J. Bacteriol. 169, 26–32.
Vemuri, G.N., Eiteman, M.A., Altman, E., 2006. Increased recombinant protein production in *Escherichia coli* strains with overexpressed water-forming NADH oxidase and a deleted ArcA regulatory protein. Biotechnol. Bioeng. 94, 538–542.
Verstrepen, K.J., Van Laere, S.D., Vanderhaegen, B.M., Derdelinckx, G., Dufour, J.P., Pretorius, I.S., Winderickx, J., Thevelein, J.M., Delvaux, F.R., 2003. Expression levels of the yeast alcohol acetyltransferase genes *ATF1, Lg-ATF1*, and *ATF2* control the formation of a broad range of volatile esters. Appl. Environ. Microbiol. 69, 5228–5237.
Wehrens, M., Ershov, D., Rozendaal, R., Walker, N., Schultz, D., Kishony, R., Levin, P.A., Tans, S.J., 2018. Size laws and division ring dynamics in filamentous *Escherichia coli* cells. Curr. Biol. 28, 972–979 e5.
Wong, I., Atsumi, S., Huang, W.C., Wu, T.Y., Hanai, T., Lam, M.L., Tang, P., Yang, J., Liao, J.C., Ho, C.M., 2010. An agar gel membrane-PDMS hybrid microfluidic device for long term single cell dynamic study. Lab Chip 10, 2710–2719.
Xu, X., Williams, T.C., Divne, C., Pretorius, I.S., Paulsen, I.T., 2019. Evolutionary engineering in *Saccharomyces cerevisiae* reveals a TRK1-dependent potassium influx mechanism for propionic acid tolerance. Biotechnol. Biofuels 12, 97.
Yang, D., Prabowo, C.P.S., Eun, H., Park, S.Y., Cho, I.J., Jiao, S., Lee, S.Y., 2021. *Escherichia coli* as a platform microbial host for systems metabolic engineering. Essays Biochem. https://doi.org/10.1042/EBC20200172.
Yomano, L.P., York, S.W., Ingram, L.O., 1998. Isolation and characterization of ethanol-tolerant mutants of *Escherichia coli* KO11 for fuel ethanol production. J. Ind. Microbiol. Biotechnol. 20, 132–138.